

The structure of the Krylov subspace in various preconditioned CGS algorithms

Shoji Itoh* and Masaaki Sugihara†

Abstract

An improved preconditioned conjugate gradient squared (PCGS) algorithm has recently been proposed, and it performs much better than the conventional PCGS algorithm. In this paper, the improved PCGS algorithm is verified as a coordinative to the left-preconditioned system, and it has the advantages of both the conventional and the left-PCGS; this is done by comparing, analyzing, and executing numerical examinations of various PCGS algorithms, including another improved one. We show that the direction of the preconditioned system for the CGS method is determined by the operations of α_k and β_k in the PCGS algorithm. By comparing the logical structures of these algorithms, we show that the direction of the preconditioned system can be switched by the construction and setting of the initial shadow residual vector.

1 Introduction

The conjugate gradient squared (CGS) [13] is one of various methods used to solve systems of linear equations

$$(1.1) \quad A\mathbf{x} = \mathbf{b},$$

where the coefficient matrix A of size $n \times n$ is usually nonsymmetric, \mathbf{x} is the solution vector, and \mathbf{b} is the right-hand side (RHS) vector.

The CGS is a bi-Lanczos method that belongs to the class of Krylov subspace methods. Bi-Lanczos-type methods are derived from the bi-conjugate gradient (BiCG) method [4, 10], which assumes the existence of a dual system $A^T \mathbf{x}^\sharp = \mathbf{b}^\sharp$ (we will refer to this as the “shadow system”). Bi-Lanczos-type algorithms have the advantage of requiring less memory than do Arnoldi-type algorithms, which is another class of Krylov subspace methods. Furthermore, a variety of bi-Lanczos-type algorithms, such as the bi-conjugate gradient stabilized (BiCGStab) method [15] and the generalized product-type method based on the BiCG (GPBiCG) [16], have been constructed by adopting the idea behind the derivation of the CGS. Various iterative methods, including bi-Lanczos-type algorithms, are often used following a preconditioning operation that is used to improve the properties of the linear equations. Such algorithms are called preconditioned algorithms; for example, the preconditioned CGS (PCGS). Therefore, it is very important to study the properties of the PCGS so that its performance can be improved.

Generally, the degree k of the Krylov subspace generated by A and \mathbf{r}_0 is expressed as $\mathcal{K}_k(A, \mathbf{r}_0) = \text{span}\{\mathbf{r}_0, A\mathbf{r}_0, A^2\mathbf{r}_0, \dots, A^{k-1}\mathbf{r}_0\}$, where \mathbf{r}_0 is the initial residual vector $\mathbf{r}_0 = \mathbf{b} - A\mathbf{x}_0$, and \mathbf{x}_0 is the initial guess at the solution. The Krylov subspace $\mathcal{K}_k(A, \mathbf{r}_0)$ generated by the k -th iteration forms the structure of $\mathbf{x}_k \in \mathbf{x}_0 + \mathcal{K}_k(A, \mathbf{r}_0)$, where \mathbf{x}_k is the approximate solution vector (or simply the “solution vector”). However, for a given preconditioned Krylov subspace method, there are various different algorithms that can be used for the preconditioning conversion. In such cases, the structure of the approximate solution formed by the Krylov subspace is often different for different algorithms, and the performance of these various algorithms can also differ substantially [8].

An improved PCGS algorithm has been proposed [8]. Reference [8] shows that this improved algorithm has many advantages over the conventional PCGS algorithms [1, 12, 15]. In this paper, a variety of PCGS algorithms are discussed. We begin by considering two typical PCGS algorithms, and we analyze the structure of the solution vector for each Krylov subspace. We then perform the

*Division of Science, School of Science and Engineering, Tokyo Denki University. (itosho@acm.org).

†Department of Physics and Mathematics, College of Science and Engineering, Aoyama Gakuin University.

same analysis for two improved PCGS algorithms, one of which was mentioned above [8], and the other is presented in the present paper. However, we note that it is not our purpose to propose a new algorithm, but to analyze the improved PCGS algorithms by comparing the structure of the Krylov subspace and the numerical results of four different PCGS algorithms.

In this paper, when we refer to a *preconditioned algorithm*, we mean one that uses a preconditioning operator M or a preconditioning matrix, and by *preconditioned system*, we mean one that has been converted by some operator(s) based on M . These terms never indicate the *algorithm for the preconditioning operation itself*, such as incomplete LU decomposition or by using the approximate inverse. For example, under a preconditioned system, the original linear system (1.1) becomes

$$(1.2) \quad \tilde{A}\tilde{\mathbf{x}} = \tilde{\mathbf{b}},$$

$$(1.3) \quad \tilde{A} = M_L^{-1}AM_R^{-1}, \quad \tilde{\mathbf{x}} = M_R\mathbf{x}, \quad \tilde{\mathbf{b}} = M_L^{-1}\mathbf{b},$$

with the preconditioner $M = M_L M_R$ ($M \approx A$). In this paper, the matrix and the vector under the preconditioned system are indicated by a tilde ($\tilde{\cdot}$). However, the conversions in (1.2) and (1.3) are not implemented directly; rather, we construct the preconditioned algorithm that is equivalent to solving (1.2).

This paper is organized as follows. Section 2 provides various preconditioned CGS algorithms; in particular, we consider right- and left-preconditioned systems for CGS algorithms. The improved PCGS algorithms are shown to be coordinative to the left-preconditioned system. Section 3 discusses the difference between the direction of a preconditioning conversion and the direction of a preconditioned system. We show that preconditioning conversions are congruent for PCGS algorithms, and we provide some examples in which the direction of the preconditioned system for the CGS is switched. In section 4, we present some numerical results to illustrate the convergence properties of the various PCGS algorithms discussed in section 2, and we illustrate the effect of switching the direction of the preconditioned system for the CGS algorithm in section 3. Finally, our conclusions are presented in section 5.

2 Analyses of various PCGS algorithms

In this section, four kinds of PCGS algorithms are analyzed. These PCGS algorithms can be derived as follows.

Algorithm 1. CGS under preconditioned system:

$\tilde{\mathbf{x}}_0$ is the initial guess, $\tilde{\mathbf{r}}_0 = \tilde{\mathbf{b}} - \tilde{A}\tilde{\mathbf{x}}_0$, set $\beta_{-1}^{\text{PCGS}} = 0$,

$(\tilde{\mathbf{r}}_0^\#, \tilde{\mathbf{r}}_0) \neq 0$, e.g., $\tilde{\mathbf{r}}_0^\# = \tilde{\mathbf{r}}_0$,

For $k = 0, 1, 2, \dots$, until convergence, Do:

$$\begin{aligned} \tilde{\mathbf{u}}_k &= \tilde{\mathbf{r}}_k + \beta_{k-1}^{\text{PCGS}} \tilde{\mathbf{q}}_{k-1}, \\ \tilde{\mathbf{p}}_k &= \tilde{\mathbf{u}}_k + \beta_{k-1}^{\text{PCGS}} (\tilde{\mathbf{q}}_{k-1} + \beta_{k-1}^{\text{PCGS}} \tilde{\mathbf{p}}_{k-1}), \\ \alpha_k^{\text{PCGS}} &= \frac{(\tilde{\mathbf{r}}_0^\#, \tilde{\mathbf{r}}_k)}{(\tilde{\mathbf{r}}_0^\#, \tilde{A}\tilde{\mathbf{p}}_k)}, \\ \tilde{\mathbf{q}}_k &= \tilde{\mathbf{u}}_k - \alpha_k^{\text{PCGS}} \tilde{A}\tilde{\mathbf{p}}_k, \\ \tilde{\mathbf{x}}_{k+1} &= \tilde{\mathbf{x}}_k + \alpha_k^{\text{PCGS}} (\tilde{\mathbf{u}}_k + \tilde{\mathbf{q}}_k), \\ \tilde{\mathbf{r}}_{k+1} &= \tilde{\mathbf{r}}_k - \alpha_k^{\text{PCGS}} \tilde{A}(\tilde{\mathbf{u}}_k + \tilde{\mathbf{q}}_k), \\ \beta_k^{\text{PCGS}} &= \frac{(\tilde{\mathbf{r}}_0^\#, \tilde{\mathbf{r}}_{k+1})}{(\tilde{\mathbf{r}}_0^\#, \tilde{\mathbf{r}}_k)}, \end{aligned}$$

End Do

Any preconditioned algorithm can be derived by substituting the matrix with the preconditioner for the matrix with the tilde and the vectors with the preconditioner for the vectors with the tilde.

Obviously, Algorithm 1 without the preconditioning conversion is the same as the CGS. If \tilde{A} is a symmetric matrix and $\tilde{\mathbf{r}}_0^\sharp = \tilde{\mathbf{r}}_0$, then Algorithm 1 can be adapted while maintaining its symmetric property.

The case shown in (1.3) is called *two-sided preconditioning*, the case in which $M_L = M$ and $M_R = I$ is called *left preconditioning*, and the case in which $M_L = I$ and $M_R = M$ is called *right preconditioning*, where I denotes the identity matrix. We now formally define these¹.

Definition 1 For the system and solution

$$(1.2') \quad \tilde{A}\tilde{\mathbf{x}} = \tilde{\mathbf{b}},$$

$$(1.3') \quad \tilde{A} = M_L^{-1}AM_R^{-1}, \quad \tilde{\mathbf{x}} = M_R\mathbf{x}, \quad \tilde{\mathbf{b}} = M_L^{-1}\mathbf{b},$$

we define the direction of a preconditioned system of linear equations as follows:

- The two-sided preconditioned system: Equation (1.3');
- The right-preconditioned system: $M_L = I$ and $M_R = M$ in (1.3');
- The left-preconditioned system: $M_L = M$ and $M_R = I$ in (1.3'),

where M is the preconditioner $M = M_L M_R$ ($M \approx A$), and I is the identity matrix.

Other vectors in the solving method are not preconditioned. The initial guess is given as \mathbf{x}_0 , and $\tilde{\mathbf{x}}_0 = M_R\mathbf{x}_0$.

The two-sided preconditioned system may be impracticable, but it is of theoretical interest.

The preconditioned system is different from the preconditioning conversion. There are various ways of performing a preconditioning conversion, but the direction of the preconditioned system is uniquely defined. (For example, see the preconditioning conversions (2.2) and (2.5) in Algorithm 2, section 2.1.1.)

Both the CGS and the PCGS extend the two-dimensional subspace in each iteration [2, 5]; therefore, the Krylov subspace $\mathcal{K}_{2k}(\tilde{A}, \tilde{\mathbf{r}}_0)$ generated by the k -th iteration forms the structure of

$$(2.1) \quad \tilde{\mathbf{x}}_k \in \tilde{\mathbf{x}}_0 + \mathcal{K}_{2k}(\tilde{A}, \tilde{\mathbf{r}}_0).$$

2.1 Two typical PCGS algorithms

In this subsection, we present two well-known and typical PCGS algorithms. One is a right-preconditioned system, although this is not always recognized, and the other is a left-preconditioned system. For each of these algorithms, we examine the structure of the Krylov subspace and the solution vector.

2.1.1 Conventional right-preconditioned PCGS

This PCGS algorithm has been described in many manuscripts and numerical libraries; for example, see [1, 12, 15]. It is usually derived by the following preconditioning conversion²:

$$(2.2) \quad \begin{aligned} \tilde{A} &= M_L^{-1}AM_R^{-1}, \quad \tilde{\mathbf{x}}_k = M_R\mathbf{x}_k, \quad \tilde{\mathbf{b}} = M_L^{-1}\mathbf{b}, \\ \tilde{\mathbf{r}}_k &= M_L^{-1}\mathbf{r}_k, \quad \tilde{\mathbf{r}}_0^\sharp = M_L^T\mathbf{r}_0^\flat, \quad \tilde{\mathbf{p}}_k = M_L^{-1}\mathbf{p}_k, \quad \tilde{\mathbf{u}}_k = M_L^{-1}\mathbf{u}_k, \quad \tilde{\mathbf{q}}_k = M_L^{-1}\mathbf{q}_k. \end{aligned}$$

Finally, Algorithm 2 is derived.

Algorithm 2. Conventional PCGS algorithm:

$$\begin{aligned} \mathbf{x}_0 &\text{ is the initial guess, } \mathbf{r}_0 = \mathbf{b} - A\mathbf{x}_0, \quad \text{set } \beta_{-1} = 0, \\ (\tilde{\mathbf{r}}_0^\sharp, \tilde{\mathbf{r}}_0) &= (\mathbf{r}_0^\flat, \mathbf{r}_0) \neq 0, \text{ e.g., } \mathbf{r}_0^\flat = \mathbf{r}_0, \end{aligned}$$

¹ Here, we have offered a general definition. However, for preconditioned bi-Lanczos-type algorithms, additional restrictions are necessary [9].

²In this case, the initial shadow residual vector (ISRV) $\tilde{\mathbf{r}}_0^\sharp$ is converted to $M_L^T\mathbf{r}_0^\flat$, but there is no problem with displaying $M_L^T\mathbf{r}_0^\flat$ in the notation of the algorithm. However, its internal structure is $\mathbf{r}_0^\flat \equiv M^{-T}\mathbf{r}_0^\sharp$. The notation \mathbf{r}_0^\flat will be discussed in section 3. The same applies to (2.5).

For $k = 0, 1, 2, \dots$, until convergence, Do:

$$\begin{aligned}
\mathbf{u}_k &= \mathbf{r}_k + \beta_{k-1} \mathbf{q}_{k-1}, \\
\mathbf{p}_k &= \mathbf{u}_k + \beta_{k-1} (\mathbf{q}_{k-1} + \beta_{k-1} \mathbf{p}_{k-1}), \\
\alpha_k &= \frac{(\mathbf{r}_0^b, \mathbf{r}_k)}{(\mathbf{r}_0^b, AM^{-1} \mathbf{p}_k)}, \\
\mathbf{q}_k &= \mathbf{u}_k - \alpha_k AM^{-1} \mathbf{p}_k, \\
\mathbf{x}_{k+1} &= \mathbf{x}_k + \alpha_k M^{-1} (\mathbf{u}_k + \mathbf{q}_k), \\
\mathbf{r}_{k+1} &= \mathbf{r}_k - \alpha_k AM^{-1} (\mathbf{u}_k + \mathbf{q}_k), \\
\beta_k &= \frac{(\mathbf{r}_0^b, \mathbf{r}_{k+1})}{(\mathbf{r}_0^b, \mathbf{r}_k)},
\end{aligned} \tag{2.3}$$

End Do

The stopping criterion is

$$\frac{\|\mathbf{r}_{k+1}\|}{\|\mathbf{b}\|} \leq \varepsilon. \tag{2.4}$$

The results of this algorithm can also be derived by the following conversion:

$$\begin{aligned}
\tilde{A} &= AM^{-1}, \quad \tilde{\mathbf{x}}_k = M \mathbf{x}_k, \quad \tilde{\mathbf{b}} = \mathbf{b}, \\
\tilde{\mathbf{r}}_k &= \mathbf{r}_k, \quad \tilde{\mathbf{r}}_0^\# = \mathbf{r}_0^b, \quad \tilde{\mathbf{p}}_k = \mathbf{p}_k, \quad \tilde{\mathbf{u}}_k = \mathbf{u}_k, \quad \tilde{\mathbf{q}}_k = \mathbf{q}_k.
\end{aligned} \tag{2.5}$$

This is the same as using $M_L = I$ and $M_R = M$ in (2.2). Furthermore, this is the same as converting only \tilde{A} , $\tilde{\mathbf{x}}_k$, and $\tilde{\mathbf{b}}$, that is, the right-preconditioned system.

2.1.2 Left-preconditioned CGS

The following conversion can be used to derive another PCGS algorithm:

$$\begin{aligned}
\tilde{A} &= M^{-1}A, \quad \tilde{\mathbf{x}}_k = \mathbf{x}_k, \quad \tilde{\mathbf{b}} = M^{-1}\mathbf{b}, \\
\tilde{\mathbf{r}}_k &= \mathbf{r}_k^+, \quad \tilde{\mathbf{r}}_0^\# = \mathbf{r}_0^\#, \quad \tilde{\mathbf{p}}_k = \mathbf{p}_k^+, \quad \tilde{\mathbf{u}}_k = \mathbf{u}_k^+, \quad \tilde{\mathbf{q}}_k = \mathbf{q}_k^+.
\end{aligned} \tag{2.6}$$

This is the same as applying $M_L = M$ and $M_R = I$ to \tilde{A} , $\tilde{\mathbf{x}}_k$, and $\tilde{\mathbf{b}}$, that is, the left-preconditioned system.

Algorithm 3. Left-preconditioned CGS algorithm (Left-PCGS):

\mathbf{x}_0 is the initial guess, $\mathbf{r}_0^+ = M^{-1}(\mathbf{b} - A\mathbf{x}_0)$, set $\beta_{-1} = 0$,

$(\tilde{\mathbf{r}}_0^\#, \tilde{\mathbf{r}}_0) = (\mathbf{r}_0^\#, \mathbf{r}_0^+) \neq 0$, e.g., $\mathbf{r}_0^\# = \mathbf{r}_0^+$,

For $k = 0, 1, 2, \dots$, until convergence, Do:

$$\begin{aligned}
\mathbf{u}_k^+ &= \mathbf{r}_k^+ + \beta_{k-1} \mathbf{q}_{k-1}^+, \\
\mathbf{p}_k^+ &= \mathbf{u}_k^+ + \beta_{k-1} (\mathbf{q}_{k-1}^+ + \beta_{k-1} \mathbf{p}_{k-1}^+), \\
\alpha_k &= \frac{(\mathbf{r}_0^\#, \mathbf{r}_k^+)}{(\mathbf{r}_0^\#, M^{-1}A\mathbf{p}_k^+)}, \\
\mathbf{q}_k^+ &= \mathbf{u}_k^+ - \alpha_k M^{-1}A\mathbf{p}_k^+, \\
\mathbf{x}_{k+1} &= \mathbf{x}_k + \alpha_k (\mathbf{u}_k^+ + \mathbf{q}_k^+), \\
\mathbf{r}_{k+1}^+ &= \mathbf{r}_k^+ - \alpha_k M^{-1}A (\mathbf{u}_k^+ + \mathbf{q}_k^+), \\
\beta_k &= \frac{(\mathbf{r}_0^\#, \mathbf{r}_{k+1}^+)}{(\mathbf{r}_0^\#, \mathbf{r}_k^+)},
\end{aligned}$$

End Do

In this paper, \mathbf{r}_k^+ denotes the residual vector under the left-preconditioned system³, its internal structure is $\mathbf{r}_k^+ \equiv M^{-1}\mathbf{r}_k$, and this is the definition of \mathbf{r}_k^+ . Note that \mathbf{p}_k^+ , \mathbf{u}_k^+ , and \mathbf{q}_k^+ achieve the same purpose. Here, \mathbf{r}_k^+ in Algorithm 3 provides different information to the residual vector $\mathbf{r}_k = \mathbf{b} - A\mathbf{x}_k$, and the stopping criterion is

$$(2.7) \quad \frac{\|\mathbf{r}_{k+1}^+\|}{\|M^{-1}\mathbf{b}\|} \leq \varepsilon.$$

Note that this is also different from (2.4), and this is an example of incomplete judging, because \mathbf{r}_{k+1}^+ never provides important information about $\mathbf{b} - A\mathbf{x}_k$. It may be thought that this is a minor issue, but in a previous paper, we observed that the left-preconditioned system can result in a serious problem (see [7], and Appendix A).

This algorithm can also be derived by the following conversion:

$$(2.8) \quad \begin{aligned} \tilde{A} &= M_L^{-1}AM_R^{-1}, \quad \tilde{\mathbf{x}}_k = M_R\mathbf{x}_k, \quad \tilde{\mathbf{b}} = M_L^{-1}\mathbf{b}, \\ \tilde{\mathbf{r}}_k &= M_R\mathbf{r}_k^+, \quad \tilde{\mathbf{r}}_0^\# = M_R^{-T}\mathbf{r}_0^\#, \quad \tilde{\mathbf{p}}_k = M_R\mathbf{p}_k^+, \quad \tilde{\mathbf{u}}_k = M_R\mathbf{u}_k^+, \quad \tilde{\mathbf{q}}_k = M_R\mathbf{q}_k^+. \end{aligned}$$

If $M_L = M$ and $M_R = I$ are substituted into (2.8), then (2.6) is obtained.

2.1.3 Comparison between two typical PCGS algorithms

Here, we compare the conventional PCGS (Algorithm 2) with the left-PCGS (Algorithm 3); we will focus on the structures of their Krylov subspaces and their solution vectors.

The conventional PCGS (Algorithm 2) is the right-preconditioned system⁴, that is, $(AM^{-1})(M\mathbf{x}) = \mathbf{b}$, and $\mathbf{r}_k = \mathbf{b} - (AM^{-1})(M\mathbf{x}_k)$. The relation between the Krylov subspace and the solution vector is

$$(2.9) \quad M\mathbf{x}_k \in M\mathbf{x}_0 + \mathcal{K}_{2k}^R(AM^{-1}, \mathbf{r}_0).$$

This means that the Krylov subspace $\mathcal{K}_{2k}^R(AM^{-1}, \mathbf{r}_0)$ generates the solution vector as $M\mathbf{x}_k$, not \mathbf{x}_k directly, but \mathbf{x}_k is calculated with corrections, as in (2.3) in Algorithm 2.

The left-PCGS (Algorithm 3) is $M^{-1}A\mathbf{x} = M^{-1}\mathbf{b}$, $\mathbf{r}_k^+ = M^{-1}(\mathbf{b} - A\mathbf{x}_k)$. The relation between its Krylov subspace and the solution vector is

$$(2.10) \quad \mathbf{x}_k \in \mathbf{x}_0 + \mathcal{K}_{2k}^L(M^{-1}A, \mathbf{r}_0^+).$$

Therefore, the Krylov subspace $\mathcal{K}_{2k}^L(M^{-1}A, \mathbf{r}_0^+)$ generates the solution vector directly as \mathbf{x}_k (Algorithm 3).

These are summarized in Table 1.

It is important to note that the structures are different for the two Krylov subspaces, $\mathcal{K}_{2k}^R(AM^{-1}, \mathbf{r}_0)$ for the conventional PCGS (the right system) and $\mathcal{K}_{2k}^L(M^{-1}A, \mathbf{r}_0^+)$ for the left-PCGS, because their scalar parameters α_k and β_k are not equivalent [8, 9]. We summarize this below; for details, see [9]. The recurrence relations of the BiCG under the preconditioned system are

$$(2.11) \quad \begin{aligned} R_0(\tilde{\lambda}) &= 1, \quad P_0(\tilde{\lambda}) = 1, \\ R_k(\tilde{\lambda}) &= R_{k-1}(\tilde{\lambda}) - \alpha_{k-1}^{\text{PBiCG}} \tilde{\lambda} P_{k-1}(\tilde{\lambda}), \end{aligned}$$

$$(2.12) \quad P_k(\tilde{\lambda}) = R_k(\tilde{\lambda}) + \beta_{k-1}^{\text{PBiCG}} P_{k-1}(\tilde{\lambda}).$$

Here, $R_k(\tilde{\lambda})$ is the degree k of the residual polynomial, and $P_k(\tilde{\lambda})$ is the degree k of the probing direction polynomial, that is, $\tilde{\mathbf{r}}_k = R_k(\tilde{A})\tilde{\mathbf{r}}_0$ and $\tilde{\mathbf{p}}_k = P_k(\tilde{A})\tilde{\mathbf{r}}_0$. For example, in the left-PBiCG, (2.11) is shown as $R_k^L(\tilde{\lambda}) = R_{k-1}^L(\tilde{\lambda}) - \alpha_{k-1}^L \tilde{\lambda} P_{k-1}^L(\tilde{\lambda})$, so $\tilde{\mathbf{r}}_k \in \mathcal{K}_{k+1}^L(\tilde{A}, \tilde{\mathbf{r}}_0)$.

³The notation \mathbf{r}_k^+ will be discussed in sections 2.1.3, 2.3, and 3, but there is no problem with displaying \mathbf{r}_k in the notation of the algorithm. Note that this is also true for \mathbf{p}_k^+ , \mathbf{u}_k^+ , and \mathbf{q}_k^+ .

⁴ The Krylov subspace of the right-preconditioned system is denoted with a superscript R, and that of the left-PCGS is denoted with a superscript L.

Table 1: Summary of two typical PCGS algorithms.

	Structure of residual vector	Structure of solution vector for each Krylov subspace
Conventional (Alg. 2)	$\mathbf{r}_k = \mathbf{b} - (AM^{-1})(M\mathbf{x}_k)$	$M\mathbf{x}_k \in M\mathbf{x}_0 + \mathcal{K}_{2k}^R(AM^{-1}, \mathbf{r}_0)$
Left-PCGS (Alg. 3)	$\mathbf{r}_k^+ = M^{-1}(\mathbf{b} - A\mathbf{x}_k)$	$\mathbf{x}_k \in \mathbf{x}_0 + \mathcal{K}_{2k}^L(M^{-1}A, \mathbf{r}_0^+)$

2.2 Improved preconditioned CGS algorithms

An improved PCGS algorithm has been proposed [8]. This algorithm retains some mathematical properties that are associated with the CGS derivation from the BiCG method under a non-preconditioned system. The improved PCGS algorithm from [8] will be referred to as ‘‘Improved1.’’ Another improved PCGS algorithm will be presented, and it will be referred to as ‘‘Improved2.’’ We note that Improved2 is mathematically equivalent to Improved1. The stopping criterion for both algorithms is (2.4).

2.2.1 The Improved1 PCGS algorithm (Improved1) [8]

Improved1 can be derived from the following conversion:

$$(2.13) \quad \begin{aligned} \tilde{A} &= M_L^{-1}AM_R^{-1}, \quad \tilde{\mathbf{x}}_k = M_R\mathbf{x}_k, \quad \tilde{\mathbf{b}} = M_L^{-1}\mathbf{b}, \\ \tilde{\mathbf{r}}_k &= M_L^{-1}\mathbf{r}_k, \quad \tilde{\mathbf{r}}_0^\# = M_R^{-T}\mathbf{r}_0^\#, \quad \tilde{\mathbf{p}}_k = M_R\mathbf{p}_k^+, \quad \tilde{\mathbf{u}}_k = M_R\mathbf{u}_k^+, \quad \tilde{\mathbf{q}}_k = M_R\mathbf{q}_k^+. \end{aligned}$$

Algorithm 4. Improved PCGS algorithm (Improved1):

\mathbf{x}_0 is the initial guess, $\mathbf{r}_0 = \mathbf{b} - A\mathbf{x}_0$, set $\beta_{-1} = 0$,

$(\tilde{\mathbf{r}}_0^\#, \tilde{\mathbf{r}}_0) = (\mathbf{r}_0^\#, M^{-1}\mathbf{r}_0) \neq 0$, e.g., $\mathbf{r}_0^\# = M^{-1}\mathbf{r}_0$,

For $k = 0, 1, 2, \dots$, until convergence, Do:

$$\begin{aligned} \mathbf{u}_k^+ &= M^{-1}\mathbf{r}_k + \beta_{k-1}\mathbf{q}_{k-1}^+, \\ \mathbf{p}_k^+ &= \mathbf{u}_k^+ + \beta_{k-1}(\mathbf{q}_{k-1}^+ + \beta_{k-1}\mathbf{p}_{k-1}^+), \\ \alpha_k &= \frac{(\mathbf{r}_0^\#, M^{-1}\mathbf{r}_k)}{(\mathbf{r}_0^\#, M^{-1}A\mathbf{p}_k^+)}, \\ \mathbf{q}_k^+ &= \mathbf{u}_k^+ - \alpha_k M^{-1}A\mathbf{p}_k^+, \\ \mathbf{x}_{k+1} &= \mathbf{x}_k + \alpha_k(\mathbf{u}_k^+ + \mathbf{q}_k^+), \\ \mathbf{r}_{k+1} &= \mathbf{r}_k - \alpha_k A(\mathbf{u}_k^+ + \mathbf{q}_k^+), \\ \beta_k &= \frac{(\mathbf{r}_0^\#, M^{-1}\mathbf{r}_{k+1})}{(\mathbf{r}_0^\#, M^{-1}\mathbf{r}_k)}. \end{aligned}$$

End Do

2.2.2 Improved2 PCGS algorithm (Improved2)

Improved2 can be derived from the following conversion:

$$(2.14) \quad \begin{aligned} \tilde{A} &= M_L^{-1}AM_R^{-1}, \quad \tilde{\mathbf{x}}_k = M_R\mathbf{x}_k, \quad \tilde{\mathbf{b}} = M_L^{-1}\mathbf{b}, \\ \tilde{\mathbf{r}}_k &= M_L^{-1}\mathbf{r}_k, \quad \tilde{\mathbf{r}}_0^\# = M_R^{-T}\mathbf{r}_0^\#, \quad \tilde{\mathbf{p}}_k = M_L^{-1}\mathbf{p}_k, \quad \tilde{\mathbf{u}}_k = M_L^{-1}\mathbf{u}_k, \quad \tilde{\mathbf{q}}_k = M_L^{-1}\mathbf{q}_k. \end{aligned}$$

Note that this conversion is different than (2.13) for $\tilde{\mathbf{p}}_k$, $\tilde{\mathbf{u}}_k$, and $\tilde{\mathbf{q}}_k$.

Algorithm 5. Another improved PCGS algorithm (Improved2):

\mathbf{x}_0 is the initial guess, $\mathbf{r}_0 = \mathbf{b} - A\mathbf{x}_0$, set $\beta_{-1} = 0$,
 $(\tilde{\mathbf{r}}_0^\#, \tilde{\mathbf{r}}_0) = (\mathbf{r}_0^\#, M^{-1}\mathbf{r}_0) \neq 0$, e.g., $\mathbf{r}_0^\# = M^{-1}\mathbf{r}_0$,
 For $k = 0, 1, 2, \dots$, until convergence, Do:

$$\begin{aligned} \mathbf{u}_k &= \mathbf{r}_k + \beta_{k-1}\mathbf{q}_{k-1}, \\ \mathbf{p}_k &= \mathbf{u}_k + \beta_{k-1}(\mathbf{q}_{k-1} + \beta_{k-1}\mathbf{p}_{k-1}), \\ \alpha_k &= \frac{(M^{-T}\mathbf{r}_0^\#, \mathbf{r}_k)}{(M^{-T}\mathbf{r}_0^\#, AM^{-1}\mathbf{p}_k)}, \\ \mathbf{q}_k &= \mathbf{u}_k - \alpha_k AM^{-1}\mathbf{p}_k, \\ \mathbf{x}_{k+1} &= \mathbf{x}_k + \alpha_k M^{-1}(\mathbf{u}_k + \mathbf{q}_k), \\ \mathbf{r}_{k+1} &= \mathbf{r}_k - \alpha_k AM^{-1}(\mathbf{u}_k + \mathbf{q}_k), \\ \beta_k &= \frac{(M^{-T}\mathbf{r}_0^\#, \mathbf{r}_{k+1})}{(M^{-T}\mathbf{r}_0^\#, \mathbf{r}_k)}, \end{aligned}$$

End Do

2.3 Analysis of the four kinds of PCGS algorithms

We will now analyze and compare the four PCGS algorithms presented above.

We split the residual vector of the left-PCGS (Algorithm 3) \mathbf{r}_k^+ into

$$(2.15) \quad \mathbf{r}_k^+ \mapsto M^{-1}\mathbf{r}_k, \quad (k = 0, 1, 2, \dots)$$

and give the necessary deformations; then, the left-PCGS (Algorithm 3) is reduced to Improved1 (Algorithm 4). Alternatively, we can derive Algorithm 3 from Algorithm 4 by substituting $M^{-1}\mathbf{r}_k$ for \mathbf{r}_k^+ , that is, $\mathbf{r}_k^+ \equiv M^{-1}\mathbf{r}_k$. By this means, we can explain the relationships between the four kinds of PCGS algorithms, as shown in Figure 1.

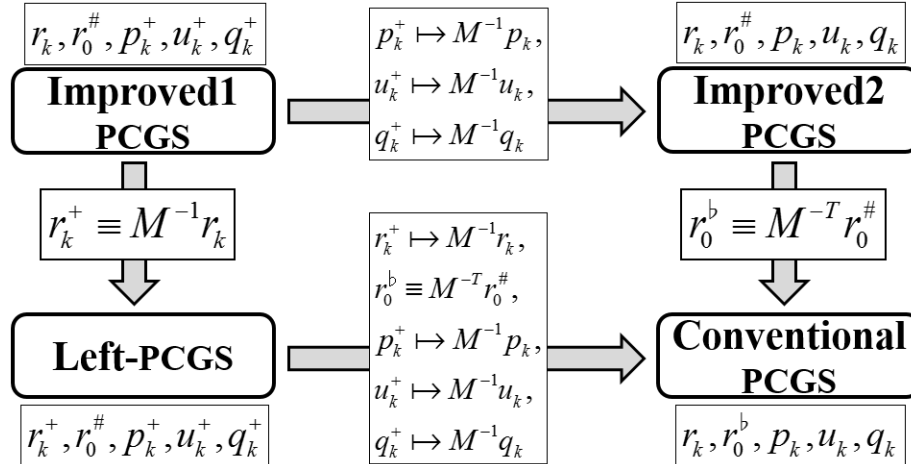


Figure 1: Relations between the four different PCGS algorithms. \mapsto : Splitting left vector to right members (preconditioner and vector), \equiv : Substituting left vector for right members.

In addition, if we apply (2.15) to (2.10) to obtain the structure of the Krylov subspace of Algorithm 3, then

$$\mathcal{K}_{2k}^L(M^{-1}A, \mathbf{r}_0^+) \mapsto \mathcal{K}_{2k}^L(M^{-1}A, M^{-1}\mathbf{r}_0) = M^{-1}\mathcal{K}_{2k}^L(AM^{-1}, \mathbf{r}_0).$$

The structure of the solution vector for the Krylov subspace is then

$$(2.16) \quad \mathbf{x}_k \in \mathbf{x}_0 + \mathcal{K}_{2k}^L(M^{-1}A, \mathbf{r}_0^+) \mapsto \mathbf{x}_k \in \mathbf{x}_0 + M^{-1}\mathcal{K}_{2k}^L(AM^{-1}, \mathbf{r}_0).$$

Here, the reason why the Krylov subspace is denoted as \mathcal{K}_{2k}^L , despite the preconditioned matrix being AM^{-1} in the right-hand summation of (2.16), is as following; the direction of a preconditioned system is different from the direction of a preconditioning conversion; see section 3.

Therefore, the system of Improved1 (Algorithm 4) is coordinative to that of the left-PCGS (Algorithm 3), and Improved2 (Algorithm 5) is equivalent to Improved1. Both algorithms have important advantages over the left-PCGS, because their residual vector is \mathbf{r}_k , and their stopping criterion is (2.4), not $\|\mathbf{r}_{k+1}^+\|/\|M^{-1}\mathbf{b}\|$.

Table 2 shows the structure of the residual vector and the structure of the solution vector for the Krylov subspace for each of the four PCGS algorithms.

Table 2: Summary of the four PCGS algorithms.

	Structure of residual vector	Structure of solution vector for each Krylov subspace
Conventional (Alg. 2)	$\mathbf{r}_k = \mathbf{b} - (AM^{-1})(M\mathbf{x}_k)$	$M\mathbf{x}_k \in M\mathbf{x}_0 + \mathcal{K}_{2k}^R(AM^{-1}, \mathbf{r}_0)$
Left-PCGS (Alg. 3)	$\mathbf{r}_k^+ = M^{-1}(\mathbf{b} - A\mathbf{x}_k)$	$\mathbf{x}_k \in \mathbf{x}_0 + \mathcal{K}_{2k}^L(M^{-1}A, \mathbf{r}_0^+)$
Improved1 (Alg. 4)	$M^{-1}\mathbf{r}_k =$	$\mathbf{x}_k \in \mathbf{x}_0 + M^{-1}\mathcal{K}_{2k}^L(AM^{-1}, \mathbf{r}_0)$
Improved2 (Alg. 5)	$M^{-1}(\mathbf{b} - (AM^{-1})(M\mathbf{x}_k))$	

In this summary, we see that the structures of the Krylov subspaces differ:

$$(2.17) \quad \mathcal{K}_{2k}^R(AM^{-1}, \mathbf{r}_0) \neq \mathcal{K}_{2k}^L(AM^{-1}, \mathbf{r}_0).$$

That is, $\mathcal{K}_{2k}^R(AM^{-1}, \mathbf{r}_0)$ of the conventional PCGS (right-preconditioned) system is different from $\mathcal{K}_{2k}^L(AM^{-1}, \mathbf{r}_0)$ of both improved PCGS (coordinative to the left-preconditioned) systems, because the scalar parameters α_k and β_k are not equivalent [8, 9]. Note that (2.17) will be confirmed in section 3, and be shown numerically in section 4.

Furthermore, superficially, the solution vector for both the conventional PCGS (Algorithm 2) and Improved2 (Algorithm 5) have the same recurrence relation: $\mathbf{x}_{k+1} = \mathbf{x}_k + \alpha_k M^{-1}(\mathbf{u}_k + \mathbf{q}_k)$. However, each recurrence relation belongs to a different system, because the components of the conventional PCGS are α_k^R , \mathbf{u}_k^R , and \mathbf{q}_k^R , and those of Improved2 are α_k^L , \mathbf{u}_k^L , and \mathbf{q}_k^L .

The structure of the residual vector of Improved1 (Algorithm 4) and Improved2 (Algorithm 5) appears as $M^{-1}\mathbf{r}_k = M^{-1}(\mathbf{b} - (AM^{-1})(M\mathbf{x}_k))$ in Table 2, because they are both from the left-PCGS and the structure of their Krylov subspace is $M^{-1}\mathcal{K}_{2k}^L(AM^{-1}, \mathbf{r}_0)$.

3 Congruence of preconditioning conversion, and direction of preconditioned system for the CGS

In the previous section, we defined the general direction of a preconditioned system for CGS (see Definition 1). However, the direction of a preconditioned system is different from the direction of a preconditioning conversion. We will show that the direction of a preconditioned system is switched by the construction of the ISRV.

3.1 Congruence of preconditioning conversion for the PCGS

Here, we consider the congruence of a preconditioning conversion for the PCGS in the following proposition.

Proposition 1 (Congruency) *There is congruence to a PCGS algorithm in the direction of the preconditioning conversion.*

Proof We have already shown instances of this. For example, Algorithm 2 can be derived by the two-sided conversion (2.2), and if $M_L = I$, $M_R = M$, and the conversion (2.2) is reduced to (2.5), then Algorithm 2 is derived. If $M_L = M$ and $M_R = I$, then Algorithm 2 can be derived. The other preconditioned algorithms (Algorithms 3, 4, and 5) and their corresponding preconditioning conversions are also the same. \square

Although this property has been repeatedly discussed in the literature, it should be considered when evaluating the direction of a preconditioned system.

3.2 Direction of a preconditioned system and that of the PCGS

The direction of a preconditioned system is different from the direction of a preconditioning conversion.

Proposition 2 *The direction of a preconditioned system is determined by the operations of α_k and β_k in each PCGS algorithm. These intrinsic operations are based on biorthogonality and biconjugacy.*

Proof The operations of biorthogonality and biconjugacy in each PCGS algorithm and the structure of the solution vector for each Krylov subspace are shown below. The underlined inner products are the actual descriptions for each PCGS algorithm.

Only the conventional PCGS (Algorithm 2) algorithm has the ISRV in the form \mathbf{r}_0^b ; in all other algorithms, it is \mathbf{r}_0^\sharp . The ISRV \mathbf{r}_0^b never splits into $M^{-T}\mathbf{r}_0^\sharp$ in this algorithm, and the preconditioned coefficient matrix for the biconjugacy is fixed as AM^{-1} , that is, the right-preconditioned system.

- Conventional (Algorithm 2) :

$$\begin{aligned}\mathbf{r}_0^b &= \mathbf{r}_0, \\ (\tilde{\mathbf{r}}_0^\sharp, \tilde{\mathbf{r}}_k) &= \left(M_L^T \mathbf{r}_0^b, M_L^{-1} \mathbf{r}_k \right) = \underline{\left(\mathbf{r}_0^b, \mathbf{r}_k \right)}, \\ (\tilde{\mathbf{r}}_0^\sharp, \tilde{A}\tilde{\mathbf{p}}_k) &= \left(M_L^T \mathbf{r}_0^b, (M_L^{-1}AM_R^{-1})(M_L^{-1}\mathbf{p}_k) \right) = \underline{\left(\mathbf{r}_0^b, (AM^{-1})\mathbf{p}_k \right)}, \\ M\mathbf{x}_k &\in M\mathbf{x}_0 + \mathcal{K}_{2k}^R(AM^{-1}, \mathbf{r}_0).\end{aligned}$$

- Left-PCGS (Algorithm 3) :

$$\begin{aligned}\mathbf{r}_0^\sharp &= \mathbf{r}_0^+, \\ (\tilde{\mathbf{r}}_0^\sharp, \tilde{\mathbf{r}}_k) &= \underline{\left(\mathbf{r}_0^\sharp, \mathbf{r}_k^+ \right)}, \\ (\tilde{\mathbf{r}}_0^\sharp, \tilde{A}\tilde{\mathbf{p}}_k) &= \underline{\left(\mathbf{r}_0^\sharp, (M^{-1}A)\mathbf{p}_k^+ \right)}, \\ \mathbf{x}_k &\in \mathbf{x}_0 + \mathcal{K}_{2k}^L(M^{-1}A, \mathbf{r}_0^+).\end{aligned}$$

- Improved1 (Algorithm 4) :

$$\begin{aligned}\mathbf{r}_0^\sharp &= M^{-1}\mathbf{r}_0, \\ (\tilde{\mathbf{r}}_0^\sharp, \tilde{\mathbf{r}}_k) &= \left(M_R^{-T}\mathbf{r}_0^\sharp, M_L^{-1}\mathbf{r}_k \right) = \underline{\left(\mathbf{r}_0^\sharp, M^{-1}\mathbf{r}_k \right)}, \\ (\tilde{\mathbf{r}}_0^\sharp, \tilde{A}\tilde{\mathbf{p}}_k) &= \left(M_R^{-T}\mathbf{r}_0^\sharp, (M_L^{-1}AM_R^{-1})(M_R\mathbf{p}_k^+) \right) = \underline{\left(\mathbf{r}_0^\sharp, (M^{-1}A)\mathbf{p}_k^+ \right)}, \\ \mathbf{x}_k &\in \mathbf{x}_0 + M^{-1}\mathcal{K}_{2k}^L(AM^{-1}, \mathbf{r}_0).\end{aligned}$$

- Improved2 (Algorithm 5) :

$$\begin{aligned}\mathbf{r}_0^\sharp &= M^{-1}\mathbf{r}_0, \\ (\tilde{\mathbf{r}}_0^\sharp, \tilde{\mathbf{r}}_k) &= \left(M_R^{-T}\mathbf{r}_0^\sharp, M_L^{-1}\mathbf{r}_k \right) = \underline{\left(M^{-T}\mathbf{r}_0^\sharp, \mathbf{r}_k \right)} = \left(\mathbf{r}_0^\sharp, M^{-1}\mathbf{r}_k \right), \\ (\tilde{\mathbf{r}}_0^\sharp, \tilde{A}\tilde{\mathbf{p}}_k) &= \left(M_R^{-T}\mathbf{r}_0^\sharp, (M_L^{-1}AM_R^{-1})(M_L^{-1}\mathbf{p}_k) \right) \\ &= \underline{\left(M^{-T}\mathbf{r}_0^\sharp, A(M^{-1}\mathbf{p}_k) \right)} = \left(\mathbf{r}_0^\sharp, (M^{-1}A)(M^{-1}\mathbf{p}_k) \right), \\ \mathbf{x}_k &\in \mathbf{x}_0 + M^{-1}\mathcal{K}_{2k}^L(AM^{-1}, \mathbf{r}_0). \quad \square\end{aligned}$$

We present the following proposition and corollary.

Proposition 3 *On the structure of biorthogonality $(\tilde{\mathbf{r}}_0^\#, \tilde{\mathbf{r}}_k)$ in the iterated part of each PCGS algorithm, there exists a single preconditioning operator between \mathbf{r}_k (basic form of the residual vector) and $\mathbf{r}_0^\#$ (basic form of the ISRV) such that M^{-1} operates on \mathbf{r}_k or M^{-T} operates on $\mathbf{r}_0^\#$.*

Proof We split $\mathbf{r}_0^b \mapsto M^{-T}\mathbf{r}_0^\#$ and $\mathbf{r}_k^+ \mapsto M^{-1}\mathbf{r}_k$ in Algorithms 2 to 5, and obtain

$$\begin{aligned} (\tilde{\mathbf{r}}_0^\#, \tilde{\mathbf{r}}_k) &= \underline{(\mathbf{r}_0^b, \mathbf{r}_k)} \mapsto (M^{-T}\mathbf{r}_0^\#, \mathbf{r}_k), \\ (\tilde{\mathbf{r}}_0^\#, \tilde{\mathbf{r}}_k) &= \underline{(\mathbf{r}_0^\#, \mathbf{r}_k^+)} \mapsto (\mathbf{r}_0^\#, M^{-1}\mathbf{r}_k), \\ (\tilde{\mathbf{r}}_0^\#, \tilde{\mathbf{r}}_k) &= \underline{(\mathbf{r}_0^\#, M^{-1}\mathbf{r}_k)}, \\ (\tilde{\mathbf{r}}_0^\#, \tilde{\mathbf{r}}_k) &= \underline{(M^{-T}\mathbf{r}_0^\#, \mathbf{r}_k)} = (\mathbf{r}_0^\#, M^{-1}\mathbf{r}_k). \end{aligned}$$

The underlined inner products are the actual descriptions for each PCGS algorithm.

In addition, for the two-sided conversion, we obtain

$$(\tilde{\mathbf{r}}_0^\#, \tilde{\mathbf{r}}_k) = (M_R^{-T}\mathbf{r}_0^\#, M_L^{-1}\mathbf{r}_k) = (M^{-T}\mathbf{r}_0^\#, \mathbf{r}_k) = (\mathbf{r}_0^\#, M^{-1}\mathbf{r}_k). \quad \square$$

Corollary 1 *On the structure of biconjugacy $(\tilde{\mathbf{r}}_0^\#, \tilde{A}\tilde{\mathbf{p}}_k)$ in the iterated part of each PCGS algorithm, there exists a single preconditioning operator between A (coefficient matrix) and $\mathbf{r}_0^\#$ (basic form of the ISRV), such that M^{-1} operates on A or M^{-T} operates on $\mathbf{r}_0^\#$. Furthermore, there exists a single preconditioning operator between A and \mathbf{p}_k (basic form of probing direction vector).*

From Propositions 2 and 3 and Corollary 1, the intrinsic operations on the biorthogonality and the biconjugacy for the four PCGS algorithms have the same matrix and vector structures, even though the superficial descriptions of these algorithms are different.

3.3 ISRV switches the direction of the preconditioned system for the CGS

Although the mathematical properties of the conventional PCGS (Algorithm 2) and Improved2 (Algorithm 5) are quite different, the structures of these algorithms are very similar. This can be seen by replacing $M^{-T}\mathbf{r}_0^\#$ with \mathbf{r}_0^b in Algorithm 5, and in the initial part, we have

$$(3.1) \quad \begin{aligned} (\tilde{\mathbf{r}}_0^\#, \tilde{\mathbf{r}}_0) &= (M_R^{-T}\mathbf{r}_0^\#, M_L^{-1}\mathbf{r}_0) = (M^{-T}\mathbf{r}_0^\#, \mathbf{r}_0) \\ &\equiv (\mathbf{r}_0^b, \mathbf{r}_0) \neq 0, \quad \text{e.g., } \mathbf{r}_0^b = \mathbf{r}_0; \end{aligned}$$

then Algorithm 5 becomes Algorithm 2.

Theorem 1 *The direction of a preconditioned system for the CGS is switched by the construction and setting of the ISRV.*

Proof Proposition 2 shows that the direction of a preconditioned system for the CGS algorithm is determined by the structures of the biorthogonality and the biconjugacy. Here, we show that their structures are switched by the ISRV. The underlined inner products are the actual operators for each PCGS algorithm.

- ISRV1 : $\mathbf{r}_0^\# = M^{-1}\mathbf{r}_0$ (Based on left conversion)

$$(3.2) \quad \begin{aligned} (\tilde{\mathbf{r}}_0^\#, \tilde{\mathbf{r}}_0) &= (M_R^{-T}\mathbf{r}_0^\#, M_L^{-1}\mathbf{r}_0) = (\mathbf{r}_0^\#, M^{-1}\mathbf{r}_0) \neq 0, \\ &\text{e.g., } \mathbf{r}_0^\# = M^{-1}\mathbf{r}_0. \end{aligned}$$

- ISRV2 : $\mathbf{r}_0^\sharp = M^T \mathbf{r}_0$ (Based on right conversion)

$$(3.3) \quad \begin{aligned} (\tilde{\mathbf{r}}_0^\sharp, \tilde{\mathbf{r}}_0) &= (M_R^{-T} \mathbf{r}_0^\sharp, M_L^{-1} \mathbf{r}_0) = (M^{-T} \mathbf{r}_0^\sharp, \mathbf{r}_0) \neq 0, \\ \text{e.g., } M^{-T} \mathbf{r}_0^\sharp = \mathbf{r}_0 &\rightarrow \mathbf{r}_0^\sharp = M^T \mathbf{r}_0. \end{aligned}$$

If we apply ISRV2 to Algorithm 5, then Algorithm 5 is equivalent to Algorithm 2 with $\mathbf{r}_0^b = \mathbf{r}_0$:

$$\begin{aligned} (\tilde{\mathbf{r}}_0^\sharp, \tilde{\mathbf{r}}_k) &= \underline{(M^{-T} \mathbf{r}_0^\sharp, \mathbf{r}_k)} = (\mathbf{r}_0, \mathbf{r}_k), \\ (\tilde{\mathbf{r}}_0^\sharp, \tilde{A} \tilde{\mathbf{p}}_k) &= \underline{(M^{-T} \mathbf{r}_0^\sharp, A(M^{-1} \mathbf{p}_k))} = (\mathbf{r}_0, (AM^{-1}) \mathbf{p}_k). \end{aligned}$$

Alternatively, if we apply $\mathbf{r}_0^b = M^{-T} M^{-1} \mathbf{r}_0$ (we will call this ISRV9) to Algorithm 2, then Algorithm 2 is equivalent to Algorithm 5 with ISRV1:

$$\begin{aligned} (\tilde{\mathbf{r}}_0^\sharp, \tilde{\mathbf{r}}_k) &= \underline{(\mathbf{r}_0^b, \mathbf{r}_k)} = (M^{-T}(M^{-1} \mathbf{r}_0), \mathbf{r}_k) = (M^{-1} \mathbf{r}_0, M^{-1} \mathbf{r}_k), \\ (\tilde{\mathbf{r}}_0^\sharp, \tilde{A} \tilde{\mathbf{p}}_k) &= \underline{(\mathbf{r}_0^b, (AM^{-1}) \mathbf{p}_k)} = (M^{-T}(M^{-1} \mathbf{r}_0), (AM^{-1}) \mathbf{p}_k) \\ &= (M^{-1} \mathbf{r}_0, (M^{-1} A)(M^{-1} \mathbf{p}_k)). \quad \square \end{aligned}$$

If we change Improved2 (Algorithm 5) to Improved1 (Algorithm 4), then we will obtain the same results.

In this section, we have confirmed (2.17): $\mathcal{K}_{2k}^R(AM^{-1}, \mathbf{r}_0) \neq \mathcal{K}_{2k}^L(AM^{-1}, \mathbf{r}_0)$, by Proposition 2 with Theorem 1. In the next section, Theorem 1 is verified numerically.

4 Numerical experiments

Convergence of the four PCGS algorithms of section 2 is confirmed in section 4.1 by evaluating three cases. Furthermore, in section 4.2, the ability of the ISRV to switch the direction of the preconditioned system (as discussed in section 3.3) is verified, as well as Theorem 1.

4.1 Comparison of the four PCGS algorithms

The test problems were generated by building real nonsymmetric matrices corresponding to linear systems taken from the University of Florida Sparse Matrix Collection [3] and the Matrix Market [11]. The RHS vector \mathbf{b} of (1.1) was generated by setting all elements of the exact solution vector $\mathbf{x}_{\text{exact}}$ to 1.0 and substituting this into (1.1). The solution algorithm was implemented using the sequential mode of the Lis numerical computation library (version 1.1.2 [14]) in double precision, with the compiler options registered in the Lis “Makefile.” Furthermore, we set the initial solution to $\mathbf{x}_0 = \mathbf{0}$. The maximum number of iterations was set to 1000.

The numerical experiments were executed on a Dell Precision T7400 (Intel Xeon E5420, 2.5 GHz CPU, 16 GB RAM) running the Cent OS (kernel 2.6.18) and the Intel icc 10.1, ifort 10.1 compiler.

In all tests, ILU(0) was adopted as the preconditioning operation for each of the PCGS algorithms; here, the value “zero” means the *fill-in* level. The ISRVs were set as $\mathbf{r}_0^b = \mathbf{r}_0$ in the conventional PCGS (Algorithm 2), $\mathbf{r}_0^\sharp = \mathbf{r}_0^+$ in the left-PCGS (Algorithm 3), and $\mathbf{r}_0^\sharp = M^{-1} \mathbf{r}_0$ in Improved1 and Improved2 (Algorithms 4 and 5, respectively)⁵.

We considered the following three cases:

- Evaluating the algorithm relative residual (see Figure 2, 5, and Table 3);
- Evaluating the true relative residual (see Figure 3, 6, and Table 4);

when we have prior knowledge of the exact solution ($\mathbf{x}_{\text{exact}}$);

- Evaluating the true relative error (see Figure 4, 7, and Table 5).

⁵ Improved2 was implemented as the conventional PCGS with $\mathbf{r}_0^b = M^{-T} M^{-1} \mathbf{r}_0$ (ISRV9).

We adopted the following stopping criteria: For case (a), we adopted the 2-norm of (2.4) for Algorithms 2, 4, and 5, and we adopted the 2-norm of (2.7) for Algorithm 3. For case (b), we adopted $\|\mathbf{b} - A\mathbf{x}_{k+1}\|_2 / \|\mathbf{b}\|_2 \leq \varepsilon$ for all algorithms. For case (c), we adopted $\|\mathbf{x}_{k+1} - \mathbf{x}_{\text{exact}}\|_2 / \|\mathbf{x}_{\text{exact}}\|_2 \leq \varepsilon$ for all algorithms. We set $\varepsilon = 10^{-12}$ for all cases.

We will first focus on the results of the conventional PCGS (Algorithm 2), as shown in Tables 3 to 5. Breakdown occurs for `jpwh_991`, and stagnation occurs for `olm5000` at pitifully insufficient accuracy⁶, although the other three algorithms (Algorithms 3 to 5) were able to solve them. Note that the disadvantages of the conventional PCGS have already been shown in [8], and Appendix A.

Next, we focus on the results of the left-PCGS (Algorithm 3), as shown in Table 3. The accuracies of `olm5000` and `watt__1` were highest for the four PCGS algorithms, but this has no theoretical underpinning, because these high accuracies occur by using the stopping criterion (2.7): $\|\mathbf{r}_{k+1}^+\|_2 / \|M^{-1}\mathbf{b}\|_2$. In many cases, the left-PCGS algorithm causes the problem of superficial convergence; see Appendix A.

Table 3: (a) Numerical evaluation using the relative residual of each algorithm. N is the problem size, and NNZ is the number of nonzero elements. The three numbers in each row for the column for each method are as follows: the leftmost number is the true relative residual \log_{10} 2-norm, the number in parentheses is the number of iterations required to reach convergence, and the lower number is the true relative error \log_{10} 2-norm.

Matrix	N	NNZ	Conventional (Algorithm 2)	Left-PCGS (Algorithm 3)	Improved1 (Algorithm 4)	Improved2 (Algorithm 5)
add32	4960	19848	-12.17 (35) -12.17	-13.06 (37) -12.96	-12.04 (35) -11.96	-12.04 (35) -11.96
bfwa782	782	7514	-9.36 (93) -10.29	-12.37 (83) -12.09	-12.82 (78) -12.48	-12.17 (84) -12.22
jpwh_991	991	6027	Breakdown	-11.83 (15) -12.10	-12.44 (16) -12.53	-12.44 (16) -12.53
olm5000	5000	19996	-0.18 (Stag.) 4.22	-12.79 (38) -10.64	-12.20 (34) -8.05	-12.21 (33) -8.00
poisson3Db	85623	2374949	-10.14 (122) -10.33	-12.93 (119) -13.31	-12.49 (123) -13.39	-11.79 (117) -12.07
sherman4	1104	3786	-12.69 (34) -13.83	-11.68 (32) -12.82	-12.69 (33) -13.82	-12.69 (33) -13.83
wang4	26068	177196	-12.22 (52) -10.14	-10.96 (55) -9.66	-12.69 (56) -9.71	-12.70 (56) -9.71
watt__1	1856	11360	-13.01 (27) -5.96	-15.48 (41) -12.63	-12.11 (35) -9.77	-12.11 (35) -9.77

⁶ The row marked `olm5000` in all tables contains the results after 1000 iterations; furthermore, `olm5000` by Algorithm 2 stagnated after 5000 iterations, due to the size of the matrix.

Table 4: (b) Numerical evaluation using the true relative residual of each algorithm.

Matrix	N	NNZ	Conventional (Algorithm 2)	Left-PCGS (Algorithm 3)	Improved1 (Algorithm 4)	Improved2 (Algorithm 5)
add32	4960	19848	-12.17 (35) -12.17	-12.04 (35) -11.96	-12.04 (35) -11.96	-12.04 (35) -11.96
bfwa782	782	7514	-9.36 (Stag.) -10.29	-12.37 (83) -12.09	-12.82 (78) -12.48	-12.17 (84) -12.22
jpwh_991	991	6027	Breakdown	-12.44 (16) -12.53	-12.44 (16) -12.53	-12.44 (16) -12.53
olm5000	5000	19996	-0.18 (Stag.) 4.22	-12.49 (31) -8.28	-12.20 (34) -8.05	-12.21 (33) -8.00
poisson3Db	85623	2374949	-10.14 (Stag.) -10.33	-12.08 (113) -12.95	-12.49 (123) -13.39	-11.77 (Stag.) -12.06
sherman4	1104	3786	-12.69 (34) -13.83	-12.68 (33) -13.81	-12.69 (33) -13.82	-12.69 (33) -13.83
wang4	26068	177196	-12.22 (52) -10.14	-12.69 (56) -9.71	-12.69 (56) -9.71	-12.70 (56) -9.71
watt_1	1856	11360	-13.01 (27) -5.96	-12.11 (35) -9.77	-12.11 (35) -9.77	-12.11 (35) -9.77

Table 5: (c) Numerical evaluation using the true relative error of each algorithm.

Matrix	N	NNZ	Conventional (Algorithm 2)	Left-PCGS (Algorithm 3)	Improved1 (Algorithm 4)	Improved2 (Algorithm 5)
add32	4960	19848	-12.17 (35) -12.17	-12.00 (36) -12.29	-12.00 (36) -12.29	-12.00 (36) -12.29
bfwa782	782	7514	-9.36 (Stag.) -10.29	-12.37 (83) -12.09	-12.00 (77) -12.42	-12.17 (84) -12.22
jpwh_991	991	6027	Breakdown	-11.83 (15) -12.10	-11.83 (15) -12.10	-11.83 (15) -12.10
olm5000	5000	19996	-0.18 (Stag.) 4.22	-12.79 (Stag.) -11.23	-12.80 (49) -13.22	-12.59 (52) -13.09
poisson3Db	85623	2374949	-10.14 (Stag.) -10.33	-11.24 (111) -12.21	-11.61 (117) -12.57	-11.53 (116) -12.04
sherman4	1104	3786	-12.69 (34) -13.83	-11.68 (32) -12.82	-11.68 (32) -12.82	-11.68 (32) -12.82
wang4	26068	177196	-12.48 (Stag.) -10.66	-13.37 (68) -12.20	-12.80 (66) -12.57	-12.83 (66) -12.17
watt_1	1856	11360	-18.06 (41) -12.13	-14.28 (40) -12.02	-14.26 (40) -12.01	-14.26 (40) -12.05

Next, it is very important to compare cases (a) and (b) (Tables 3 and 4) with case (c) (Table 5), in order to determine the crucial ways in which they differ. Because (a) and (b) can be evaluated without knowing the exact solution but (c) requires the exact solution, it is important to examine the results when the exact solution is known. Comparing the results for `bfwa782`, `poisson3Db`, and `watt_1` in cases (a) and (b) (Tables 3 and 4), the conventional PCGS (Algorithm 2) has results in which the true relative residual or true relative error (or both) is much less accurate than those obtained by the other algorithms, and only in the conventional PCGS does stagnation occur at insufficient accuracy⁷. In particular, the conventional PCGS is the fastest to converge for `watt_1`

⁷ The results of `poisson3Db` with Improved2 in Table 4 and `olm5000` with the left-PCGS in Table 5 can be considered to be sufficiently accurate, because they had nearly converged to within 10^{-12} . We note that $\varepsilon = 10^{-12}$ is a stringent value for the tolerance for the true relative residual and the true relative error.

in cases (a) and (b) (Tables 3 and 4), but this is undesirable, because when convergence occurs too quickly, the relative residual and the true relative residual may fail to meet the criterion for accuracy. On the other hand, based on the true relative error in case (c) (Table 5), we see that the conventional PCGS converges after almost the same number of iterations as do the other methods.

Next, in contrast, the results of the conventional PCGS with `wang4` gave the most accurate true relative error for cases (a) and (b) (Tables 3 and 4), but the conventional PCGS stagnated with `wang4`, and this resulted in the lowest accuracy for case (c) (Table 5).

From the graphs in Figures 2 to 7, we can see the following: in case (a), Improved1, Improved2, and the left-PCGS show different convergence behaviors, but in cases (b) and (c), they show similar behaviors. These results correspond to the analysis in section 2.3. Therefore, Algorithms 4 and 5 are coordinative to Algorithm 3 regarding the structures of the solution vector for the generated Krylov subspace, in spite of the difference between the residual vectors: \mathbf{r}_k^+ for the left-PCGS (Algorithm 3) and \mathbf{r}_k for Improved1 and Improved2 (Algorithms 4 and 5, respectively). The conventional PCGS had a convergence behavior that differs from those of all of the other algorithms for cases (a) to (c).

These numerical results conform to the behavior expected from the discussion of the relation between the structure of the solution vector and the Krylov subspace. We compared the numerical results with the theoretical results of sections 2.1.3 and 2.3, and these are summarized as follows:

1. For case (a), the difference between the residual vector \mathbf{r}_k^+ of the left-PCGS and \mathbf{r}_k has been verified.
2. For cases (b) and (c), we verified (2.16):

$$\mathbf{x}_k \in \mathbf{x}_0 + \mathcal{K}_{2k}^L(M^{-1}A, \mathbf{r}_0^+) \mapsto \mathbf{x}_k \in \mathbf{x}_0 + M^{-1}\mathcal{K}_{2k}^L(AM^{-1}, \mathbf{r}_0).$$
Further, we verified (2.17): $\mathcal{K}_{2k}^R(AM^{-1}, \mathbf{r}_0) \neq \mathcal{K}_{2k}^L(AM^{-1}, \mathbf{r}_0).$
3. The differences between the conventional PCGS, the left-PCGS, Improved1, and Improved2 have been confirmed through examining their convergence behavior. That is, we considered the relation of the solution vector and the Krylov subspace between the right system (the conventional PCGS) and the left-PCGS, and between the coordinative PCGSs and the left-PCGS (Improved1 and Improved2).

4.2 Behavior of the PCGS when it is switched by the ISRV

In this subsection, the experimental environment was the same as that described in section 4.1, except that we used Matlab 7.8.0 (R2009a), and we gave different ISRVs to the conventional PCGS and Improved1.

We compared five different PCGS algorithms, including using a different ISRV. In the figures, we use the following labels: “Conventional” means the conventional PCGS (Algorithm 2), for which the ISRV is $\mathbf{r}_0^b = \mathbf{r}_0$; this is a right-preconditioned system. “Impr1-ISRV1” means Improved1 (Algorithm 4) with ISRV1: $\mathbf{r}_0^\sharp = M^{-1}\mathbf{r}_0$. “Impr1-ISRV2” means Improved1 with ISRV2: $\mathbf{r}_0^\sharp = M^T\mathbf{r}_0$. “Left” means the left-PCGS (Algorithm 3), for which the ISRV is $\mathbf{r}_0^+ = \mathbf{r}_0^+$. “Conv_ISRV9” means the conventional PCGS with ISRV9: $\mathbf{r}_0^b = M^{-T}M^{-1}\mathbf{r}_0$.

The convergence histories of “Conventional,” “Impr1-ISRV1,” and “Left” in Figures 8 and 9 are the same as those of “Conventional,” “Improved1,” and “Left-PCGS,” respectively, in Figures 3 and 6.

In both figures, “Impr1-ISRV2” and “Conv_ISRV9” were added to verify Theorem 1. The convergence history of “Impr1-ISRV2” is the same as that of “Conventional,” and those of “Impr1-ISRV1” and “Conv_ISRV9” are the same as that of “Left.”

We have numerically verified the claims of section 3; in particular, we have verified Theorem 1.

5 Conclusions

In this paper, an improved PCGS algorithm [8] has been analyzed by mathematically comparing four different PCGS algorithms, and we have focused on the structures of their Krylov subspace and the solution vector. From our analysis and numerical results, we have verified two improved PCGS algorithms. They are both coordinative to the left-preconditioned systems, although their residual vector maintains the basic form \mathbf{r}_k , not \mathbf{r}_k^+ . For both algorithms, the structures of the Krylov

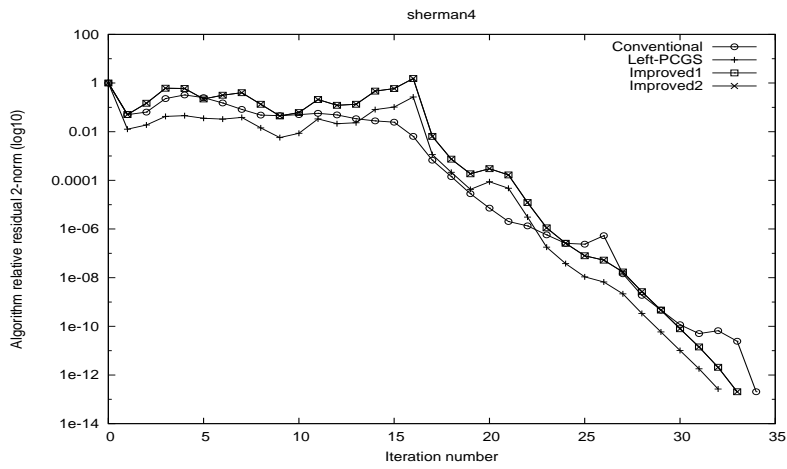


Figure 2: (a) Convergence history of the algorithm relative residual 2-norm for each of the four algorithms (sherman4).

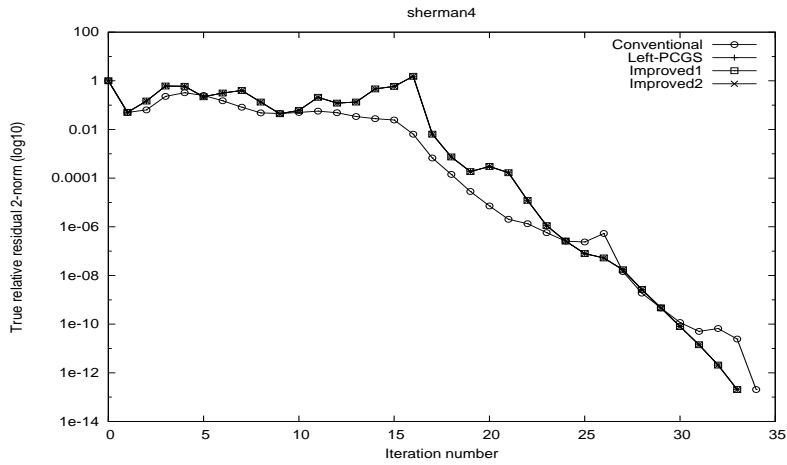


Figure 3: (b) Convergence history of the true relative residual 2-norms (sherman4) for each of the four algorithms.

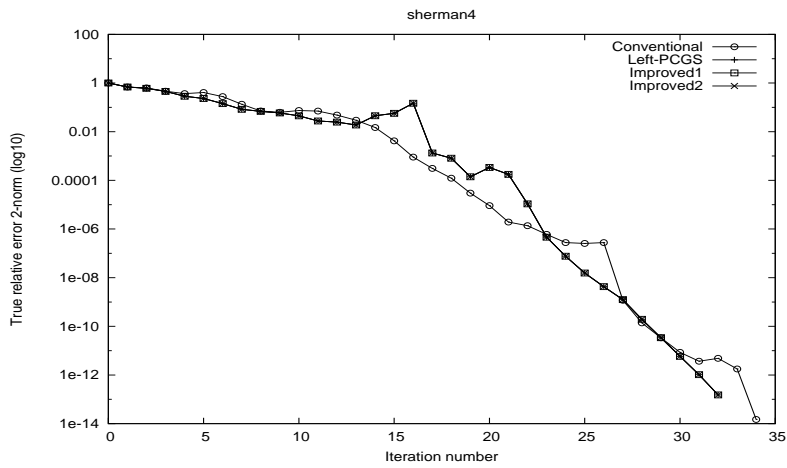


Figure 4: (c) Convergence history of the true relative error 2-norm (sherman4) for each of the four algorithms.

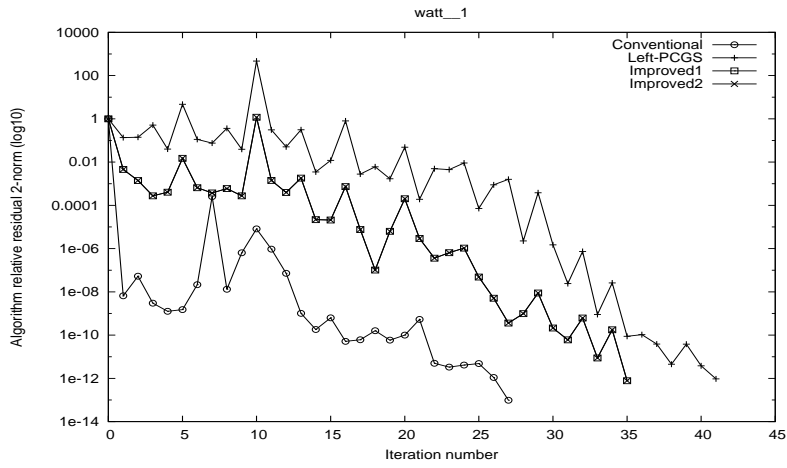


Figure 5: (a) Convergence history of the algorithm relative residual 2-norm (watt_1) for each of the four algorithms.

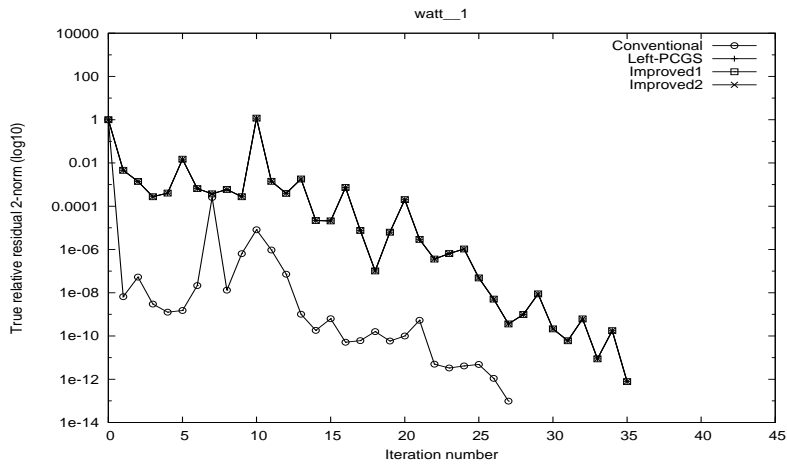


Figure 6: (b) Convergence history of the true relative residual 2-norm (watt_1) for each of the four algorithms.

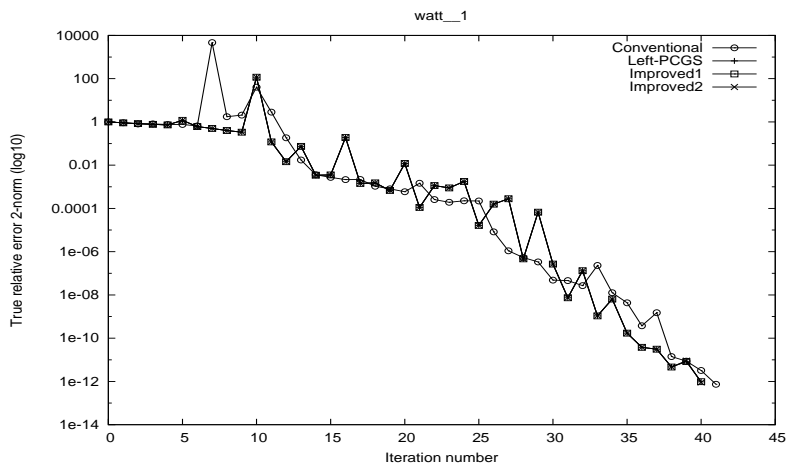


Figure 7: (c) Convergence history of the true relative error 2-norm (watt_1) for each of the four algorithms.

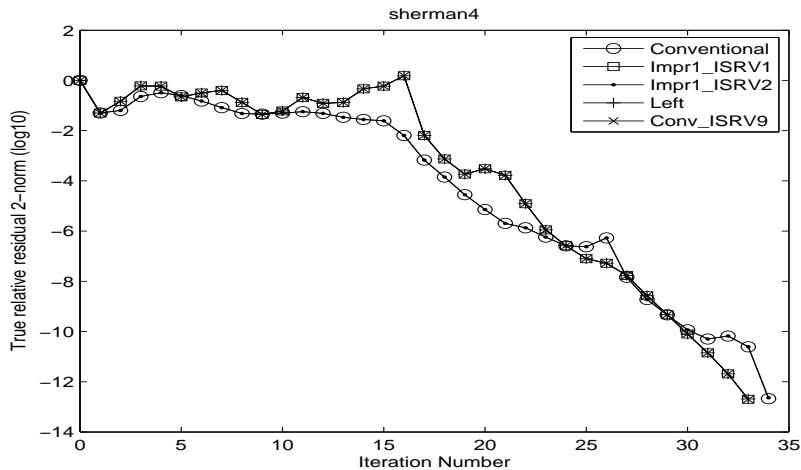


Figure 8: Convergence history of the true relative residual 2-norm of the right- and left-preconditioned PCGS, for each of the five PCGS algorithms with ISRV switching (sherman4).

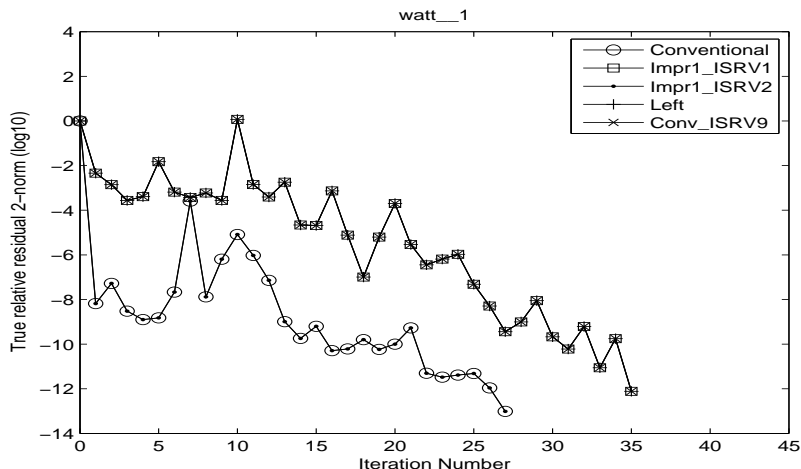


Figure 9: Convergence history of true relative residual 2-norm of the right- and left-preconditioned PCGS, for each of the five PCGS algorithms with ISRV switching (watt_1).

subspace and the solution vector are $\mathbf{x}_k \in \mathbf{x}_0 + M^{-1}\mathcal{K}_{2k}^L(AM^{-1}, \mathbf{r}_0)$. Further, the numerical results of the improved PCGS with the ILU(0) preconditioner show many advantages, such as effectiveness and consistency across several preconditioners, have also been shown; see [8] and Appendix A. We note that the improved PCGS algorithms share some of the advantages of the conventional PCGS (the right-preconditioned system) and the left-PCGS algorithms, while they avoid some of their disadvantages.

We presented a general definition of the direction of a preconditioned system of linear equations. Furthermore, we have shown that the direction of a preconditioned system for CGS is switched by the construction and setting of the ISRV. This is because the direction of the preconditioning conversion is congruent. We have also shown that the direction of a preconditioned system for CGS is determined by the operations of α_k and β_k and that these intrinsic operations are based on biorthogonality and biconjugacy. However, the structures of these intrinsic operations are the same in all four of the PCGS algorithms. Therefore, we have focused on the ability of the ISRV to switch the direction of a preconditioned system, and such a mechanism may be unique to the bi-Lanczos-type algorithms that are based on the BiCG method.

As we analyzed the four PCGS algorithms, we paid particular attention to the vectors. We note

that there exist preconditioned BiCG (PBiCG) algorithms that correspond to the preconditioning conversion of each of the PCGS algorithms. The polynomial structure of the PBiCG can be minutely analyzed by replacing the vectors of the PCGS. We have analyzed the four PBiCG algorithms in parallel [9], and each PBiCG corresponds to one of the four PCGS algorithms in this paper. In [9], using the ISRV to switch the direction of a preconditioned system was discussed in detail.

References

- [1] R. Barrett, et al., *Templates for the Solution of Linear Systems: Building Blocks for Iterative Methods*, SIAM, Philadelphia, PA, 1994.
- [2] A. M. Bruaset, *A Survey of Preconditioned Iterative Methods*, Longman Scientific & Technical, Harlow, Essex, UK, 1995.
- [3] T. A. Davis, *The University of Florida Sparse Matrix Collection*, <http://www.cise.ufl.edu/research/sparse/matrices/>
- [4] R. Fletcher, *Conjugate gradient methods for indefinite systems*, in Numerical Analysis: Proceedings of the Dundee Conference on Numerical Analysis, 1975, G. Watson, ed., Lecture Notes in Math. 506, Springer, New York, pp. 73–89, 1976.
- [5] M. H. Gutknecht, *On Lanczos-type methods for Wilson fermions*, in Numerical Challenges in Lattice Quantum Chromodynamics, A. Frommer, T. Lippert, B. Medeke, and K. Schilling, eds., Lecture Notes in Computational Science and Engineering 15, Springer, Berlin, pp. 48–65, 2000.
- [6] M. R. Hestenes and E. Stiefel, *Methods of conjugate gradients for solving linear systems*, J. Res. Nat. Bur. Standards, 49, pp. 409–435, 1952.
- [7] S. Itoh and M. Sugihara, *Systematic performance evaluation of linear solvers using quality control techniques*, in Software Automatic Tuning From Concepts to State-of-the-Art Results, K. Naono, K. Teranishi, J. Cavazos, and R. Suda, eds., Springer, New York, pp. 135–152, 2010.
- [8] S. Itoh and M. Sugihara, *Formulation of a preconditioned algorithm for the conjugate gradient squared method in accordance with its logical structure*, Appl. Math., 6, pp. 1389–1406, 2015.
- [9] S. Itoh and M. Sugihara, *The structure of the polynomials in preconditioned BiCG algorithms and the switching direction of preconditioned systems*, arXiv:1603.00175 [math.NA], 2016 .
- [10] C. Lanczos, *Solution of systems of linear equations by minimized iterations*, J. Res. Nat. Bur. of Standards, 49, pp. 33–53, 1952.
- [11] Matrix Market, <http://math.nist.gov/MatrixMarket/>
- [12] G. Meurant, *Computer Solution of Large Linear Systems*, Elsevier, New York, 2005.
- [13] P. Sonneveld, *CGS: A fast Lanczos-type solver for nonsymmetric linear systems*, SIAM J. Sci. Stat. Comput., 10, pp. 36–52, 1989.
- [14] SSI project, *Lis: Library of iterative solvers for linear systems*, <http://www.ssisc.org/lis/>
- [15] H. A. Van der Vorst, *Bi-CGSTAB: A fast and smoothly converging variant of Bi-CG for the solution of nonsymmetric linear systems*, SIAM J. Sci. Stat. Comput., 13, pp. 631–644, 1992.
- [16] S.-L. Zhang, *GPBi-CG: Generalized product-type methods based on Bi-CG for solving nonsymmetric linear systems*, SIAM J. Sci. Comput., 18, pp. 537–551, 1997.

A Systematic performance evaluation of PCGS

We consider the superficial convergence on three types of preconditioned CGS algorithms; the results shown in Figure 10 provide an overview of this weakness in the left-PCGS. The figure presents a systematic performance evaluation of solving a linear equation by three PCGS algorithms (conventional, left, and improved1) and with nine kinds of preconditioners. Here, we briefly discuss the figure; the details of a systematic performance evaluation can be found in Reference [7], which discusses the right- and the left-preconditioned systems.

The conditions of the numerical experiments presented in this appendix were almost the same as those in section 4.1 and Reference [7, section 9.2.2], except for the computational environment. The systematic performance evaluation was executed on a Hitachi HA8000 (AMD Opteron 8356; 2.3 GHz CPU; memory size: 32 GB/node) running the Red Hat Enterprise Linux 5 and the Intel icc 10.1, ifort 10.1 compiler. The maximum number of iterations was equal to the size of each matrix. The test problems were also generated as in section 4.1 and Reference [7, section 9.2.2].

Figure 10 shows the solution performance data. The rows indicate the forty-eight kinds of linear equations for the coefficient matrix names that are listed in Table 6; the columns indicate the three PCGS algorithms, each of which is subdivided into columns for the nine preconditioners.

Table 6: Real nonsymmetric matrices used for systematic performance evaluation in Figure 10.

Chebyshev{1,3}, add{20,32}, arc130, bwf782{a,b}, chem_master1, cry{10000,2500}, ecl32, epb[0-3], fs_760_[1-3], gre_{1107,115}, jpwh_991, mcca, mcf, memplus, olm{1000, 2000, 5000}, pde{2961,900}, poisson3D{a,b}, raefsky{1,2,3,5,6}, sherman[1-5], sme3Dc, torso2, viscoplastic2, watt_{1,2}, xenon{1,2}

Table 7: Number of cases of superficial convergence for each PCGS in Figure 10.

Conventional (Algorithm 2)	Left-PCGS (Algorithm 3)	Improved1 (Algorithm 4)
24	52	18

The contents of each cell are as follows. The number in each cell indicates the convergence rate⁸. A period (.) indicates that it did not converge until the maximum number of iterations, “bd” indicates that the process broke down, an asterisk (*) with a gray background indicates that the convergence was superficial convergence, and a blank indicates that it was not solved for some other reason.

Here, we consider the number of cases of superficial convergence. Superficial convergence occurs when the residual vector implies that convergence has occurred, but the solution vector is not a sufficiently accurate approximation to the true residual vector.

The stopping criteria were as follows:

$$(2.4') \quad \|\mathbf{r}_{k+1}\|_2 / \|\mathbf{b}\|_2 \leq \varepsilon, \quad (\text{Conventional and Improved1 PCGS}),$$

$$(2.7') \quad \|\mathbf{r}_{k+1}^+\|_2 / \|M^{-1}\mathbf{b}\|_2 \leq \varepsilon, \quad (\text{Left-PCGS}).$$

⁸ We based the maximum number of iterations on the size of the problem, and converted this to a percentage to obtain the convergence score. In this study, we calculate the score for when the number of iterations required for convergence is less than or equal to 20% of the matrix size, then

$$\text{score} = 10 - \left[\frac{\text{Required number of iterations (iter)} - 1}{\text{Size of the coefficient matrix (N)}} \times \text{div} \right], \quad (\text{in this study, div} = 50),$$

otherwise, score = 0. If score < 0, then score = 0. Here, [] indicates Gauss notation. If score = 10, the number of iterations required for convergence is less than or equal to 2% of the matrix size, and a lower score means slower convergence. If score = 0, the number of iterations required for convergence is greater than 20% of the matrix size [7]. Example: We solve a linear equation of matrix size N = 782. If iter = 14, 84, 148, 259, then score = 10, 5, 1, 0, respectively.

However, in this appendix, it is not our main purpose to discuss the value of the score but to compare the instances of superficial convergence (*) or other problem cases ('period', 'bd', and 'blank').

No.	Data Set			Conventional									Left-PCGS									Improved1									
	Solver	N	NNZ	03 01	03 02	03 03	03 04	03 05	03 06	03 07	03 08	03 09	03 01	03 02	03 03	03 04	03 05	03 06	03 07	03 08	03 09	03 01	03 02	03 03	03 04	03 05	03 06	03 07	03 08	03 09	
1	Chebyshev1	251	2319	.	9	.	.	.	0	.	0	.	.	8	.	.	.	0	*	0	*	.	.	8	.	.	.	0	.	.	7
2	Chebyshev3	4101	36879	.	10	10	.	.	10	10	9
3	ed320	2395	13151	8	7	9	10	8	10	10	10	9	8	7	9	10	8	10	10	10	9	8	7	9	10	8	10	10	10	9	
4	ed32	4980	19648	10	10	10	10	10	10	10	10	10	10	10	10	10	10	10	10	10	10	10	10	10	10	10	10	10	10	10	
5	arc130	130	1037	9	10	10	10	9	9	10	10	10	9	10	10	10	9	9	10	9	9	9	10	10	10	9	9	10	9	10	
6	bfw782a	782	7514	0	5	4	10	0	2	.	3	3	0	5	3	10	0	4	*	1	5	.	0	5	3	10	0	4	.	1	3
7	bfw782b	782	5982	10	10	10	10	10	10	10	10	10	10	10	10	10	10	10	10	10	10	10	10	10	10	10	10	10	10	10	
8	chem_master1	40401	201201	10	10	*	10	10	10	10
9	cny10000	10000	49699
10	cny2500	2500	12349	*	.	*	.	.	*	.	0	.	.	*	0	0
11	ed32	51993	380415	10	10	10	10	*	10	.	*	*	*	10	10	10	10	10	*	10	10	*	10	10	10	10	10	.	10	10	
12	epb0	1794	7764	*	8	8	.	*	9	.	9	8	0	8	8	.	0	9	.	9	9	0	8	7	.	0	8	.	9	8	
13	epb1	14734	95053	*	10	10	10	*	10	.	10	10	*	10	*	10	*	10	*	10	10	*	10	*	10	*	10	.	10	10	
14	epb2	25228	175027	10	10	10	.	10	10	.	10	10	10	10	10	.	10	10	*	10	10	10	10	10	.	10	10	.	10	10	
15	epb3	84617	463525	7	10	10	.	*	10	.	10	10	*	10	10	.	*	10	*	10	10	*	10	10	.	9	10	.	10	10	
16	fs_760_1	760	5739	10	10	10	10	10	10	10	10	10	10	10	10	10	10	10	10	10	10	10	10	10	10	10	10	10	10	10	
17	fs_760_2	760	5739	0	6	4	.	0	0	.	.	9	0	6	4	.	0	1	*	0	8	.	0	5	4	.	0	1	.	0	9
18	fs_760_3	760	5816	0	0	0
19	gre_1107	1107	5664	*	*
20	gre_115	115	421	*	*	.	.	.	*
21	ipwh_991	991	8027	bd	bd	bd	bd	bd	bd	bd	bd	bd	bd	10	10	*	9	9	10	10	10	bd	10	10	10	9	8	10	10	10	
22	mca	180	2659	*	9	*	.	*	*	.	8	9	*	9	*	*	*	*	*	8	9	*	9	0	.	*	0	.	7	9	
23	mefe	765	24362	*	10	*	.	*	*	.	9	10	*	10	*	.	*	*	*	9	10	.	10	*	.	*	.	.	9	10	
24	memplus	17758	99147	10	10	10	10	10	10	10	10	10	10	10	10	10	10	10	10	10	10	10	10	10	10	10	10	10	10	10	
25	alm1000	1000	3996	bd	.	.	.	10	.	8	.	.	bd	.	.	8	10	.	9	.	.	bd	.	.	8	10	
26	alm2000	2000	7996	bd	.	.	8	10	.	9	.	.	bd	.	*	10	10	.	9	7	10	
27	alm5000	5000	19996	bd	.	.	9	10	.	10	.	.	bd	.	.	9	10	.	10	.	.	bd	.	.	9	10	
28	pde2961	2961	14585	7	10	10	10	8	9	.	10	10	*	10	10	10	*	9	.	10	10	*	10	9	10	*	9	.	10	10	
29	pde900	900	4380	*	9	9	*	7	8	.	10	10	5	9	9	*	7	8	*	10	10	5	9	9	0	7	8	.	10	10	
30	paissan3Da	13514	352762	10	10	10	10	10	10	10	10	10	10	10	10	10	10	10	10	10	10	10	10	10	10	10	10	10	10	10	
31	paissan3Db	85623	2374949	*	10	10	10	*	10	10	10	10	*	10	10	10	*	10	10	10	10	*	10	10	10	*	10	10	10	10	
32	vaefsky1	3242	293409	*	10	10	.	8	9	10	10	10	*	10	10	.	8	9	10	10	10	*	10	10	.	8	9	10	10	10	
33	vaefsky2	3242	293551	1	10	9	.	4	9	10	10	10	1	10	9	.	*	8	10	10	10	*	10	9	.	*	8	10	10	10	
34	vaefsky3	21200	1488768	0	10	0	.	.	10	.	.	0	.	10	.	.	0	10	*	.	2	.	10	0	.	.	10
35	vaefsky5	8318	167178	10	10	10	10	10	10	10	10	10	10	10	10	10	10	10	10	10	10	10	10	10	10	10	10	10	10	10	
36	vaefsky6	3402	130371	10	10	10	10	10	10	10	10	10	10	10	10	10	10	10	10	10	10	10	10	10	10	10	10	10	10	10	
37	sherman1	1000	3750	0	8	5	10	1	9	7	9	10	0	8	5	10	1	9	7	9	10	0	8	5	10	1	9	7	9	10	
38	sherman2	1080	23094	.	10	0	10	.	10	*	*	10	10	.	10	0	10
39	sherman3	5005	20033	*	9	8	10	*	*	10	9	10	*	10	9	10	5	8	10	10	10	*	9	8	10	5	4	10	10	10	
40	sherman4	1104	3766	6	9	9	10	7	6	10	9	10	7	9	9	10	7	6	10	9	10	8	9	9	10	7	6	10	9	10	
41	sherman5	3312	20793	9	10	10	.	9	8	.	10	10	9	10	10	.	9	8	.	10	10	9	10	10	.	9	8	.	10	10	
42	sme3Dc	42930	3148556	.	.	9	10	.	.	10	9	10	.	.	10	*	8	10	.	.	10	.	.
43	tara2	119987	1033473	10	10	10	.	10	10	10	10	10	10	10	10	.	10	10	10	10	10	10	10	10	.	10	10	10	10	10	
44	viscoplastic2	32769	381326	9	.	10	9	9	10	*	0	9	9	10	.	0
45	watt_1	1856	11360	8	10	10	10	8	10	10	10	10	7	9	9	10	8	10	10	10	10	8	10	9	10	8	10	10	10	10	
46	watt_2	1856	11350	6	9	9	.	7	9	9	9	10	5	8	9	*	5	9	9	9	10	6	9	9	.	6	9	9	9	10	
47	xenan1	48800	1181120	9	.	10	10	9	9	10	.	.	9	.	10	10	9	9	10	.	*	.	9	.	10	10	9	9	10	.	.
48	xenan2	157484	3666668	10	.	10	10	10	10	10	.	.	10	.	10	10	10	10	10	.	*	.	10	.	10	10	10	10	10	.	.

Figure 10: Superficial convergence with three different PCGS methods and nine different preconditioners. Superficial convergence is indicated by an asterisk * with a gray background. Thick lines group columns for (from left to right) the conventional PCGS (Algorithm 2), the left-PCGS (Algorithm 3), and Improved1 (Algorithm 4). Each such frame has a cell for each of the nine preconditioners (from left to right): Point Jacobi [01], ILU(0) [02], SSOR [03], Hybrid type [04], I+S [05], SAINV [06], SA-AMG [07] (with “-saamg_unsym true” option), Crout ILU [08], and ILUT [09], where the two digits in [] indicate the identification number of the solver or preconditioner. N is the matrix size, and NNZ is the number of nonzero elements.

Here, \mathbf{r}_{k+1} and \mathbf{r}_{k+1}^+ are the residual vectors for the corresponding PCGS. When these conditions are satisfied, the numerical solution ($\hat{\mathbf{x}}_{k+1}$) is obtained, and the true relative residual is calculated as follows:

$$(A.1) \quad \|\mathbf{b} - A\hat{\mathbf{x}}_{k+1}\|_2 / \|\mathbf{b}\|_2 \leq \hat{\varepsilon}.$$

In this systematic performance evaluation, ε in (2.4') and (2.7') was set to 1.0×10^{-12} . On the other hand, $\hat{\varepsilon}$ in (A.1) was set to 1.0×10^{-8} , because $\hat{\varepsilon} = 1.0 \times 10^{-12}$ is a stringent value for the tolerance for the true relative residual. We consider that superficial convergence has occurred when (2.4') or (2.7') is satisfied, but (A.1) is not.

Figure 10 and Table 7 show that the stopping criterion (2.7') for the left-PCGS is inadequate. Therefore, the left-PCGS has a serious defect, in that superficial convergence can occur; we note that this also occurs with other left-preconditioned algorithms [7].

Just as information on Figure 10, the numbers of problem cases (not converged or not solved, breakdown, and superficial convergence) are 172, 159, and 152 for the conventional PCGS, the left-PCGS, and the improved1 PCGS, respectively.